Structure Elucidation of a Novel Aluminum Methylphosphonate, $Al_3(CH_3PO_3)_2{\cdot}O{\cdot}(OH)_3$, through a Combination of X-ray Powder Diffraction, Solid-State NMR Spectroscopy, and Computational Energy Minimization

Mark Edgar,[†] Vinton J. Carter,[†] Paramjit Grewal,[‡] Lesley-J. Sawers,[†] Enrique Sastre,[§] David P. Tunstall,[||] Paul A. Cox,[‡] Philip Lightfoot,[†] and Paul A. Wright*,[†]

School of Chemistry, University of St. Andrews, Purdie Building, St. Andrews, Fife, KY16 9ST, U.K., Centre for Molecular Design, University of Portsmouth, King Henry Building, King Henry I Street, Portsmouth, PO1 2DY, U.K., Instituto de Catalisis y Petrolequimica, CSIC, Campus Universidad Autonoma, Cantoblanco-28049, Madrid, Spain, and School of Physics, University of St. Andrews, St. Andrews, Fife, KY16 9SS, U.K.

Received December 7, 2001. Revised Manuscript Received April 25, 2002

A novel aluminum methylphosphonate, formula $Al_3(CH_3PO_3)_2{\cdot}O{\cdot}(OH)_3$, has been prepared hydrothermally. Its structure was solved by a combination of 1-D MAS NMR and 2-D five-quantum MAS NMR spectroscopies, computational energy minimization using density functional theory (DFT), and direct methods crystallographic programs tailored to X-ray powder diffraction. The structure, which crystallizes in *Pmnb* [$a = 19.7105(1)$ Å, $b = 10.1385(5)$ Å, $c = 5.1408(3)$ Å], is made up of aluminophosphonate layers lined on both sides with methyl groups. Aluminum adopts two crystallographic sites in the structure, which exhibit octahedral and distorted trigonal bipyramidal geometries. These give characteristic NMR signals ($\delta_{iso} = 10.8$ and 3.1 ppm, respectively), and their environment is accurately simulated by computational modeling.

Introduction

Metal phosphonates make up a fast-growing class of crystalline organic−inorganic hybrid solids that usually exhibit layered or framework structures. Many of these materials display good thermal stability, intercalation, and adsorption properties, and they exhibit a remarkable variety in the nature of the organic group that is covalently bound to the inorganic framework via the phosphorus. There is already an extensive literature on group IV (zirconium and titanium) phosphonates,[1−3] as well as on the phosphonates of divalent metals such as manganese[4] and zinc.[5] Group III phosphonates, including gallium,[6] indium,[7] and in particular aluminum phosphonates, have been the subject of more recent study. Aluminum phosphonates, such as aluminum methylphosphonates,[8−13] benzylphosphonates,[14,15] phenylphosphonates,[16] carboxyethylphosphonates,[17] and diphosphonates,[18] display a range of structure types based typically on layered arrangements of organic and inorganic groups in which the organic and inorganic parts of the structure are arranged in separate regions. Exceptions to this structural motif include two polymorphs of $Al_2(CH_3PO_3)_3$ (AlMePO-α and -*β*),[8−10] which have framework structures with hexagonal arrays of one-dimensional channels lined with methyl groups. The

* Correspondence to: Dr. Paul A. Wright, School of Chemistry, University of St. Andrews, Purdie Building, North Haugh, St. Andrews, Fife, KY16 9ST. Tel.: 01334 463793. Fax: 01334 463808. E-mail: paw2@st-andrews.ac.uk.

[†] School of Chemistry, University of St. Andrews.

[‡] University of Portsmouth.

[§] Instituto de Catalisis y Petrolequimica, CSIC.

[||] School of Physics, University of St. Andrews.

(1) Alberti, G.; Casciola, M. *Solid State Ionics* **1997**, *97*, 177.

(2) Alberti, G.; Casciola, M.; Costantino, U.; Vivani, R. *Adv. Mater.* **1996**, *8*, 291.

(3) Clearfield, A. Metal phosphonate chemistry. *Prog. Inorg. Chem.* **1998**, *47*, 371.

(4) Poojary, D. M.; Zhang, B. L.; Clearfield, A. *J. Am. Chem. Soc.* **1997**, *119*, 12550.

(5) Poojary, D. M.; Zhang, B. L.; Bellinghausen, P.; Clearfield, A. *Inorg. Chem.* **1996**, *35*, 5254.

(6) Bujoli-Doeuff, M.; Evain, M.; Fayon, F.; Alonso, B.; Massiot, D.; Bujoli, B. *Eur. J. Inorg. Chem.* **2000**, *12*, 2497.

(7) Morizzi, J.; Hobday, M.; Rix, C. *J. Mater. Chem.* **1999**, *9*, 863.

(8) Maeda, K.; Kiyozumi, Y.; Mizukami, F. *Angew. Chem., Int. Ed. Engl.* **1994**, *33*, 2335.

(9) Maeda, K.; Akimoto, J.; Kiyozumi, Y.; Mizukami, F. *Angew. Chem., Int. Ed. Engl.* **1995**, *34*, 1199.

(10) Maeda, K.; Akimoto, J.; Kiyozumi, Y.; Mizukami, F. *J. Chem. Soc., Chem. Commun.* **1995**, 1033.

(11) Carter, V. J.; Wright, P. A.; Gale, J. D.; Morris, R. E.; Sastre, E.; Perez-Pariente, J. *J. Mater. Chem.* **1997**, *7*, 2287.

(12) Sawers, L.-J.; Carter, V. J.; Armstrong, A. R.; Bruce, P. G.; Wright, P. A.; Gore, B. E. *J. Chem. Soc., Dalton Trans.* **1996**, 3159.

(13) Hix, G. B.; Carter, V. J.; Wragg, D. S.; Morris, R. E.; Wright, P. A. *J. Mater. Chem.* **1999**, *9*, 179.

(14) Zakowsky, N.; Hix, G. B.; Morris, R. E. *J. Mater. Chem.* **2000**, *10*, 2375.

(15) Chaplais, G.; Le Bideau, J.; Leclerq, D.; Mutin, H.; Vioux, A. *J. Mater. Chem.* **2000**, *10*, 1593.

(16) Cabeza, A.; Aranda, M. A. G.; Bruque, S.; Poojary, D. M.; Clearfield, A.; Sanz, J. *Inorg. Chem.* **1978**, *17*, 4168.

(17) Hix, G. B.; Wragg, D. S.; Wright, P. A.; Morris, R. E. *J. Chem. Soc., Dalton Trans.* **1998**, *20*, 3359.

(18) Harvey, H. G.; Teat, S. J.; Attfield, M. P. *J. Mater. Chem.* **2000**, *10*, 2632.

10.1021/cm011296q CCC: $22.00 © 2002 American Chemical Society
Published on Web 07/11/2002

structural variety in the aluminum methyl phosphonates appears to reflect the ability of aluminum to adopt a range of coordination geometries: whereas the aluminum in AlMePO-α and -β exists in both octahedral and tetrahedral coordination, it is entirely octahedral in $AlOH(CH_3PO_3) \cdot H_2O$.[13] A number of other aluminum alkylphosphonate phases of unknown structure have been observed to crystallize from hydrothermal syntheses[19] and, in this paper, we report the successful characterization of one of these phases in which the aluminum occurs in two different coordination environments. Many of these phases are prepared only as crystals of insufficient quality for single-crystal X-ray crystallography and, in these cases, X-ray powder diffraction is the most important technique in the structure solution. Although the solution of extended lattice structures from powder X-ray diffraction is far from routine, several direct methods crystallographic programs are available that have been used successfully for phosphonate structures to give a starting structural model for subsequent refinement using the Rietveld method.

For structures where only powder diffraction data are available, the models must also be shown to be consistent with other structural information, for example that from solid-state NMR and computational studies.[20,21] For aluminum phosphates and phosphonates, ^{31}P NMR spectroscopy is a powerful technique for determining the number of crystallographically distinct phosphate (or phosphonate) environments. NMR spectra of quadrupolar nuclei such as ^{27}Al are more complex than those of spin-$^1/_2$ nuclei such as ^{31}P, and it is therefore more difficult to resolve aluminum signals from very similar, but crystallographically distinct, environments. However, in structures such as those under study here, where aluminum can exist in very different coordination environments, ^{27}Al is found to be a more discriminating nucleus. This is because the chemical shift and peak shape of ^{27}Al MAS NMR signals are strongly affected by the coordination and local symmetry of the aluminum atom. The peaks are broad as a consequence of large quadrupolar coupling constants. This can lead to considerable overlap in one-dimensional spectra, but the recently developed multiple-quantum 2D MAS NMR method[22] (applicable to quadrupolar nuclei such as aluminum) permits greatly enhanced resolution. This is clear from the resolution of signals from the three different tetrahedrally coordinated aluminum species in AlMePO-β.[23] Data from single-quantum and multiple-quantum NMR ^{27}Al studies therefore provide an important constraint on any structural model that is proposed.

In addition, the final structural model should be energetically stable, as determined computationally by energy minimization methods. Very little atomistic modeling of organic−inorganic hybrids has been reported, but recent work in this area has demonstrated the validity of semiempirical and density functional theory (DFT) methods for these materials.[24] The application of these modeling methodologies to unknown materials will therefore serve not only to differentiate between suggested models but also to establish further the reliability of the method for organic−inorganic hybrid solids.

In this work, we report the hydrothermal synthesis of a novel, microcrystalline aluminum methylphosphonate [described herein as AlMePO-2, where AlMePO-1 refers to $AlOH(CH_3PO_3) \cdot H_2O$[13]] as part of ongoing studies into the synthesis and crystal chemistry of aluminum phosphonates. Chemical analyses and X-ray powder diffraction studies provided composition, unit cell dimensions, and symmetry information, and a direct methods program gave a starting model for structural studies. The ^{27}Al MAS NMR data and computer simulations indicate that, although the first model was in most respects correct, a closely related structural model was deemed more reasonable on chemical and energetic grounds and was found to be more consistent with both the ^{27}Al MAS NMR and X-ray crystallography data.

Experimental Section

AlMePO-2 was synthesized from a homogeneous gel made from aluminum hydroxide hydrate (Aldrich), methyl phosphonic acid (Avocado), and water ($Al/P/H_2O = 1.5:1:50$), which was adjusted to pH 5 using a solution of sodium hydroxide. The gel was heated to 220 °C in a PTFE-lined stainless steel autoclave, and after 2 days, the contents were filtered, washed with distilled water, and dried in air at 60 °C.

High-resolution powder X-ray diffraction data were collected using a Stoe STADI/p diffractometer in transmission mode, scanning 2θ between 5° and 90°, using monochromatic Cu $K_{\alpha 1}$ radiation [curved germanium (111)] with $\lambda = 1.540\,56$ Å. The sample was mounted between two sheets of Mylar foil. Scanning electron microscopy of the sample was performed on a JEOL JSM-5600 electron microscope, and elemental analysis was performed by energy-dispersive analysis of X-rays (EDX) on a JEOL JEM-2010 transmission electron microscope fitted with an Oxford Instruments 6498 EDX detector. X-ray fluorescence analysis was performed on a Philips PW 1450/20 X-ray spectrometer using Rh K_α radiation, and ICP-AES analysis was performed on a sample digested in concentrated hydrochloric acid. Carbon, hydrogen, and nitrogen analyses were performed using a CE Instruments EA 1110 CHNS analyzer. Thermogravimetric analysis coupled with mass spectroscopic analysis of the gases evolved was performed between 30 and 900 °C under a flow of helium.

^{31}P and ^{13}C MAS NMR spectra were recorded on a Bruker 400 spectrometer operating at 161.923 and 100.577 MHz, respectively. For ^{31}P spectra, direct polarization was used, whereas cross-polarization was used for ^{13}C spectra, and high-power proton decoupling was employed during FID detection. ^{27}Al MAS NMR spectra were recorded on a Bruker 500 spectrometer operating at 130.2 MHz, with spinning speeds of up to 9.5 kHz. 2-D 5Q (five-quantum) MAS NMR spectra were recorded on the same spectrometer using the amplitude-modulated method[25] with a *z* filter to ensure that the echo and anti-echo were combined with equal amplitudes.[22] The pulse lengths were optimized to give typical values of 4, 1.5, and 14 μs, with the pulse power of the last pulse being approximately 10% of the power of the first two. The data in the second dimension were collected for 256 experiments incremented by 5 μs. The 5Q excitation and detection are less efficient than

(19) Carter, V. J. Ph.D. Thesis, University of St. Andrews, St. Andrews, Fife, U.K., 1998.
(20) Thomas, J. M.; Vaughan, D. E. W. *J. Phys. Chem. Solids* **1989**, *50*, 449.
(21) Catlow, C. R. A.; Thomas J. M.; Freeman C. M.; Wright, P. A.; Bell, R. G. *Proc. R. Soc., London A* **1993**, *442*, 85.
(22) Amoureux, J.-P.; Fermandez, C.; Steuernagel, S. *J. Magn. Reson. Ser. A* **1996**, *123*, 116.
(23) Rocha, J.; Lin, Z.; Fernandez, C.; Amoureux, J.-P. *J. Chem. Soc., Chem. Commun.* **1996**, 2513.
(24) Grewal, P.; Cox, P. A.; Wright, P. A. **2002**, manuscript in preparation.
(25) Brown, S.; Wimperis, S. *J. Magn. Reson.* **1997**, *128*, 42.

the 3Q coherence, resulting in the need for longer experiments to attain an equivalent signal-to-noise ratio; however, 5Q spectra exhibit a significant enhancement in the resolution (a factor of 4.2 for the f1 dimension[26]), thus allowing broad signals with similar chemical shifts to be separated and analyzed. The "ridge" line-shape in these spectra has a gradient that is characteristic of the spin quantum number and the coherence order. All ^{27}Al spectra samples were calibrated to aluminum nitrate at 0 ppm. Processing was carried out using Bruker software, and spectra were simulated using SIMPSON.[27]

Crystallographic Analysis. Diffractograms were indexed using the Werner, Visser, and Louer algorithms available within the STOE WINXPOW software.[28] For ab initio structure solution, pattern decomposition was performed and approximate atom positions were located using the direct methods program EXPO[29] with structure factors extracted from reflections measured over the range $5° < 2\theta < 90°$. Refinement was performed by Rietveld refinement of the full powder diffraction profile using the GSAS suite of programs.[30] Hydrogen atoms were placed on the methyl group in a staggered conformation. Hydroxide groups were identified by bond valence calculations, but their associated hydrogens were not added to the model during refinement. Crystallographic data have been deposited with the Cambridge Crystallographic Data Centre (CCDC 185976). Copies can be obtained free of charge on application to CCDC, 12 Union Road, Cambridge, CB12 1EZ, U.K. (fax (+44) 1223-336-033, e-mail deposit@ccdc.cam.ac.uk).

Computational Methods. In this study, the structure of AlMePO-2 was modeled using a first-principles approach involving no adjustable parameters based on density functional theory (DFT), as implemented in the program CASTEP.[31] DFT[32] is a general theory that describes the total energy of a system in terms of the electron density. Plane waves are used as the basis functions, and the exchange and correlation energies of the electrons are handled by the local density approximation (LDA). Only the valence electrons are treated explicitly in the calculation, with the core electrons assumed to be in the same state in the molecule as in the free atom. The interaction between the valence electrons and the ion cores is described by pseudopotentials for each kind of atom. These pseudopotentials are generated by first-principles calculations on free atoms. The CASTEP code has been used successfully to model a wide-range of different types of systems.[33] Recent work has demonstrated that this approach can be successfully used to reproduce accurately the structures of known aluminophosphonate materials.[24]

Calculations were performed using CASTEP version 4.2 implemented on a SG Origin 2000 (Proton) at the Rutherford-Appleton Laboratory. Exchange and correlation energies were treated using the LDA approximation extended to take into account density gradients via the generalized gradient approximation (GGA). A kinetic energy cutoff of 260 eV was used, and ultrasoft potentials were used to represent the core−valence electron interactions. Geometry optimizations were performed with fixed lattice parameters and full relaxation of the internal coordinates. Convergence criteria of 0.2×10^{-4} eV atom^{-1} for the total energy, 0.001 Å for RMS displacement of atoms, and 0.05 eV atom^{-1} were imposed.

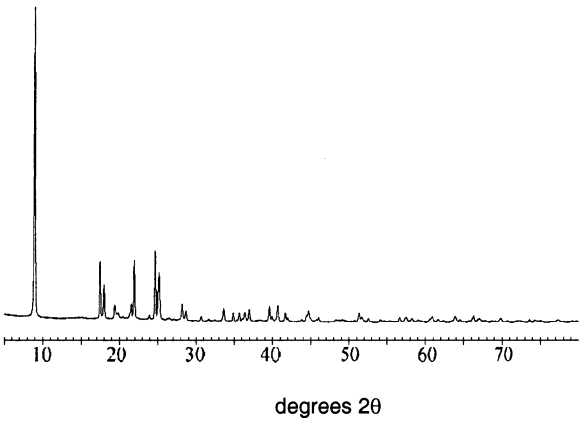

Figure 1. Powder X-ray diffraction pattern of the aluminium methylphosphonate AlMePO-2.

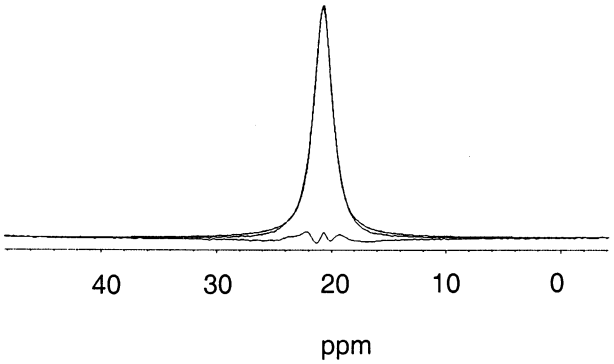

Figure 2. ^{31}P MAS NMR spectrum of AlMePO-2. The spectrum contains only a single resonance that can be fitted with a single peak, indicating that there is only one kind of methylphosphonate environment in the solid.

Results and Discussion

The X-ray diffraction pattern of the new solid (AlMePO-2) is given in Figure 1. Electron microscopy indicated that it was composed of small flat plates a few microns in size. Visual examination suggested that the sample was crystallographically quite pure, and this conclusion was supported by the X-ray diffraction studies described later. Elemental analysis by EDX on these small plates indicated that the samples had an Al/P ratio of 1.5 and indicated the presence of oxygen and carbon but no other species (there was no sodium in the sample from the added sodium hydroxide). Bulk analyses indicated that the overall Al/P ratio of the sample was between 1.66 (ICP) and 1.7 (XRF). Solid-state ^{31}P (Figure 2) and ^{13}C (not shown) MAS NMR spectra are consistent with one crystallographically distinct methylphosphonate unit being present in the solid, with no other carbon-containing species ($\delta_{\text{phosphorus}} = 20.77$ ppm; $\delta_{\text{carbon}} = 14$ ppm, split by a $^1J_{C-P}$ coupling of 158.8 Hz). ^{27}Al MAS NMR spectroscopy indicates that there are at least two kinds of aluminum in well-defined environments, typical of sites within a crystal structure, plus a broader resonance centered at 18 ppm that probably corresponds to aluminum sites in a less crystalline phase (Figure 3a). The intensity of this additional aluminum signal varies between different samples of AlMePO-2, suggesting that it arises from different amounts of this separate impurity phase in the preparations. We conclude from the difference between the selected area and the bulk analysis and from the NMR

(26) Pike, K. J.; Malde, R. P.; Ashbrook, S. E.; McManus. J.; Wimperis, S. *Solid State NMR* **2000**, *16*, 203.
(27) Bak, M.; Rasmussen, J. T.; Nielsen, N. C. *J. Magn. Reson.* **2000**, *147*, 296.
(28) *STOE WinXPOW*, ver. 1.04; STOE & Cie GmbH: Darmstadt, Germany, 1998.
(29) Altomare, A.; Burla, M. C.; Camalli, M.; Carrozzini, B.; Cascarano, G.; Giacovazzo, C.; Guagliardi, A.; Moliterni, A. G. G.; Polidori, G.; Rizzi, R. *EXPO*, release 1.03; Istituto di Ricerca per lo Sviluppo di Metodologie Cristallografiche (CNR IRMEC): Bari, Italy, 1999.
(30) Larson, A.; Von Dreele, R. Report No. LA-UR-86-748; Los Alamos National Laboratory: Los Alamos, NM, 1987.
(31) Payne, M. C.; Teter, M. P.; Allan, D. C.; Arias, T. A.; Joannopoulos, J. D. *Rev. Mod. Phys.* **1992**, *64*, 1045.
(32) Kohn, W.; Sham, L. J. *Phys. Rev. A* **1965**, *140*, 1133.
(33) Nobes, R. H.; Akhmatskaya, E. V.; Milman, V.; Winkler, B.; Pikard, C. J. *Comput. Mater. Sci.* **2000**, *17*, 141.

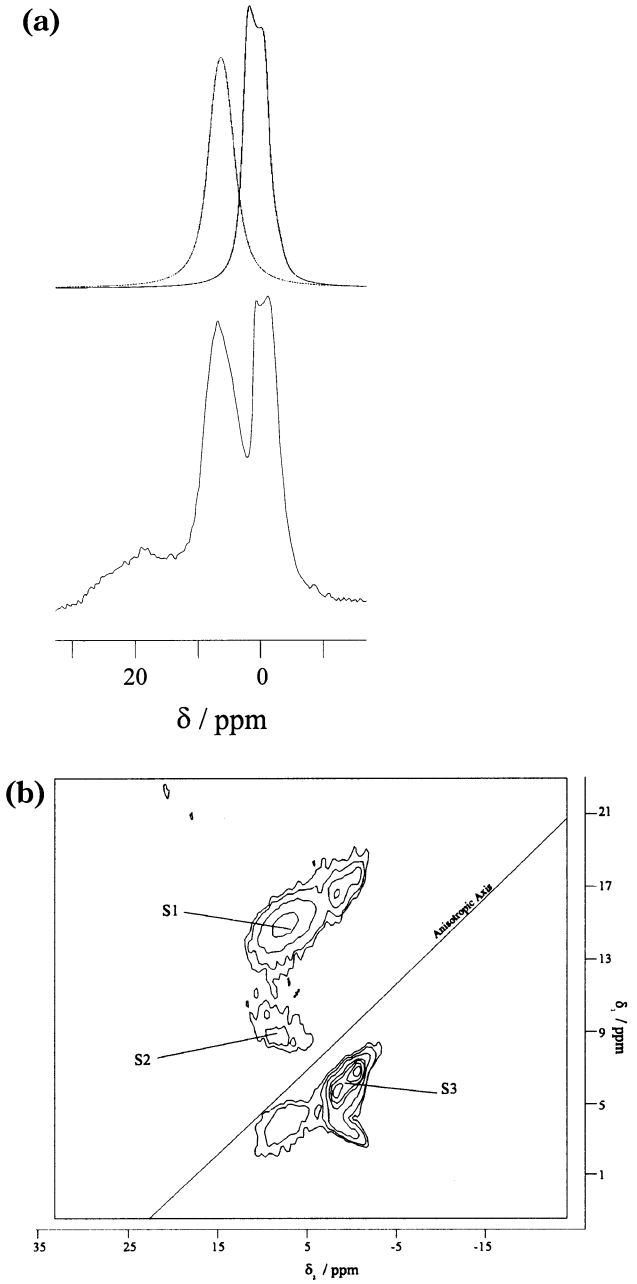

Figure 3. (a) ^{27}Al MAS NMR spectrum of AlMePO-2, indicating at least two distinct aluminum environments (top, spectrum calculated using parameters obtained from multiple-quantum experiments; bottom, experimental spectrum). (b) Five-quantum MAS NMR spectrum of AlMePO-2, showing two well-resolved aluminum environments (S1, S3) and a small impurity (S2). Estimation of true isotropic chemical shifts δ_{iso} and asymmetry of these resonances from the spectrum enables the single-quantum spectrum to be simulated accurately.

studies that the preparation is a physical mixture of a single, highly crystalline aluminum methylphosphonate phase with a small amount of a hydrated aluminum oxide phase. The latter is poorly crystalline (as shown by the X-ray diffraction results below), contains no phosphonate, and accounts for ca. 10−20% of the total aluminum in the sample.

TGA showed weight losses over three temperature ranges (Figure 4). Below 300 °C, there is a weight loss that varies between AlMePO-2 samples, with observed values of between 0.5 and 1.0%. At higher temperatures, there is a sharp loss in weight of 8.0% centered at

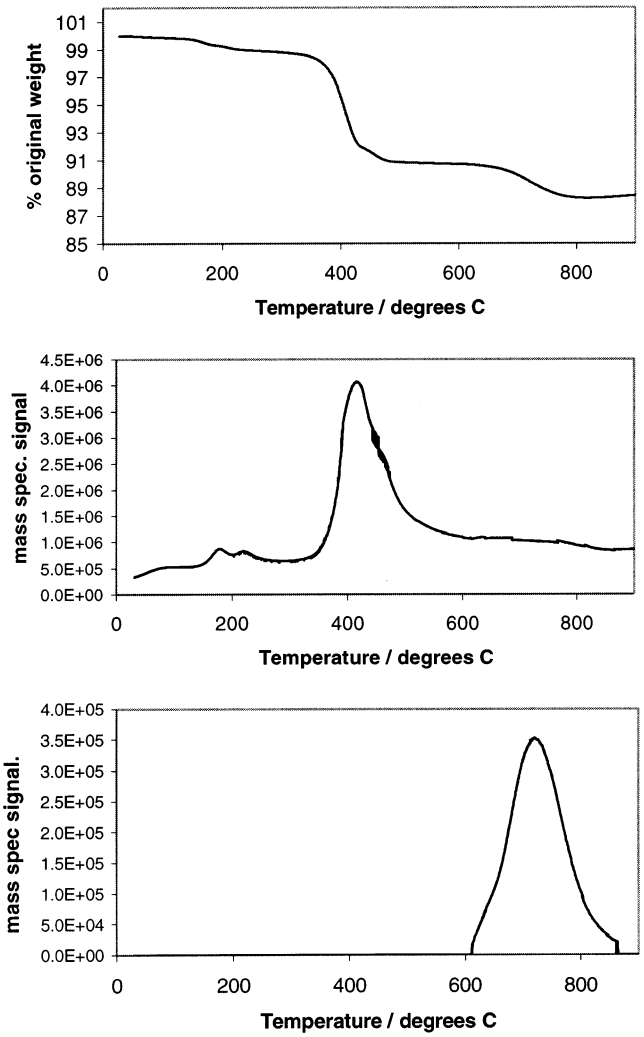

Figure 4. TG-MS results for AlMePO-2 heated at 20 °C/min in a flow of helium: weight loss curve (top) and two selected traces following the ions of $m/e = 17$ (middle) and $m/e = 15$ (bottom). The $m/e = 17$ fragment is characteristic of evolved water, whereas the $m/e = 15$ fragment is characteristic of methane.

400 °C and a third weight loss of 2.5% centered at 720 °C. After being heated to 250 °C, the solid remains crystalline, but by 600 °C, it has become amorphous. The first weight loss is shown by TG-MS to be due to loss of water (*m/e* 17, 18) and is attributed to dehydration of hydrated aluminum oxide or hydroxide impurities. The second weight loss (450 °C) is due to loss of water only (*m/e* 17, 18) and corresponds to the thermal decomposition of hydroxyl groups within the structure. (Elemental analysis for carbon after heating at 600 °C also shows no loss of carbon in this region.) The third weight loss is mainly attributable to loss of methane (*m/e* 12−16), with traces of higher hydrocarbons, although a background signal in the mass spectrum from water makes it difficult to rule out any further water loss.

Assuming that the crystalline structure must correspond to the general empirical formula $Al_3(CH_3PO_3)_2{\cdot}O_x{\cdot}(OH)_y{\cdot}(H_2O)_z$, where $2x + y = 5$ for charge balance, the most likely general formula from the analytical and TGA data is $Al_3(CH_3PO_3)_2{\cdot}O{\cdot}(OH)_3$. (The higher observed bulk Al/P ratio is explained by the presence of 10−20% of the aluminum in an impurity phase.) Loss

of all of the hydroxyl groups from the aluminum methylphosphonate compound as water (step A below) would give a predicted weight loss of 8.0 wt % (as is observed).

$$\text{step A} \quad 2Al_3(CH_3PO_3)_2{\cdot}O{\cdot}(OH)_3(s) \rightarrow 2Al_3(CH_3PO_3)_2O_5(s) + 3H_2O(g)$$

Loss of all the methyl groups as methane (leaving residual carbon) would require a weight loss of 7% of the original, which is much greater than that observed (2.5%). This means that carbonaceous residue containing hydrogen must be retained in the solid after structural collapse. The pure compound would be expected to contain 7.1 wt % C and 2.7 wt % H; the measured values of 6.7 wt % C and 2.4 wt % H are in reasonable agreement, especially considering that there is a poorly crystalline impurity.

AlMePO-2 consists of crystallites too small to be analyzed using single-crystal X-ray diffraction, even at a synchrotron source. Indexing of the X-ray powder diffraction pattern using the algorithm of Werner gave an orthorhombic cell, $a = 19.733$ Å, $b = 10.154$ Å, $c = 5.148$ Å (figure of merit 24). The space group was determined using the systematic absences to be *Pmnb* (although the noncentrosymmetric $P2_1nb$ was also considered). From the measured density (ca. 2.05 ± 0.1 g cm^{-3}), the unit cell contents using the predicted stoichiometry would be $Al_{12}(CH_3PO_3)_8{\cdot}O_4{\cdot}(OH)_{12}$ (calculated density = 2.17 g cm^{-3}).

X-ray diffraction analysis indicates that only a very few, minor diffraction maxima (total intensity of less than 1% of the total) are not taken into account by the cell and symmetry derived from indexing. With these experimental data as a guide, an initial structural model was developed by analysis of the powder X-ray diffraction pattern using the direct methods program EXPO. The positions of the heavy aluminum and phosphorus atoms were determined, and carbon and phosphonate oxygen atoms were located near the phosphorus atom, with the oxygens near the aluminums. An iterative procedure involving Rietveld refinement of the atomic positions (constraining the geometry of the carbon, phosphorus, and oxygen atoms of the phosphonate group), followed by the location of the residual electron density using difference Fourier plots, located two additional maxima, which were taken to be oxygen atoms. One of these appeared to be coordinated to three aluminum atoms; the other appeared not to be directly coordinated and was thought to be a water molecule with partial occupancy. The fit of the calculated pattern from this model to the powder X-ray data was acceptable.[19] To balance the charge of the structure, the locations of protons were estimated from bond valence calculations.[34]

The structural model was a layered arrangement of inorganic aluminophosphonate layers, covered on each side with methyl groups and stacked along the *a* axis. The aluminums are present in this model in trimeric clusters, with two aluminums tetrahedrally coordinated and one as a square pyramid, linked to each other via oxygens to give chains.[19] However, two discrepancies between this structural model and the experimental data remained. First, the TGA data are not consistent with the presence of uncoordinated water, the loss of which would be expected to occur earlier than the dehydroxylation and to give rise to a weight loss in excess of that observed. Second, the NMR chemical shift data from the ^{27}Al 1-D single-quantum spectrum would be better fitted by distorted five-fold and octahedral configurations than by tetrahedral and square-pyramidal configurations. To assess these discrepancies, computational simulations and a more detailed NMR investigation were performed.

^{27}Al MAS NMR Spectroscopy. It should, in principle, be possible to obtain the coordination environments of the two crystallographically distinct aluminums from their positions in the 1-D solid-state NMR spectrum because chemical shifts are characteristic of environment. However, the most intense part of the peak shapes in the 1-D solid-state NMR spectrum is rarely the real isotropic chemical shift (δ_{iso}). Thus, the true isotropic chemical shift cannot be obtained by simple inspection of the spectrum and must be obtained via iterative fitting or direct calculation of the FID. The observed chemical shift depends, in part, on the quadrupolar coupling constant, which, in turn, correlates to the electric field gradient around the aluminum nuclei as defined by the bonding configuration. Clearly, unusual bonding configurations such as the trigonally coordinated oxygen and distinct five-fold aluminum coordination, as well as the Al−O−Al connectivity, create atypical electric field gradients around the aluminum nuclei, making it difficult to estimate the quadrupolar coupling constants a priori. To help resolve this problem and to determine the true isotropic chemical shifts, a 2-D multiple-quantum solid-state MAS NMR spectrum was recorded. The additional resolution achieved by collection in two dimensions enabled the broad overlapping signals to be completely separated and analyzed. Resulting isotropic chemical shifts of 10.8 and 3.1 ppm ($\delta_{iso} = {}^4/_9\delta_1 + {}^5/_9\delta_2$) were extracted for the 2-D spectrum (Figure 3b). The quadrupolar coupling constant for the signal at 3.1 ppm is indicated by the splitting in this peak and was estimated to be 1.7 MHz.

The line shape also indicates that the asymmetry factor for the signal is zero ($\eta = 0$) or near-zero ($\eta \rightarrow 0$). For the signal at 10.8 ppm, it is more difficult to estimate the quadrupolar coupling constant from either the 1-D or 2-D spectrum, as the signal is broadened by an asymmetry value of approximately 0.4 that masks the classic quadrupole splitting pattern. Simple calculation provides an estimated quadrupolar coupling constant of 1.5 MHz. Using these isotropic chemical shift and asymmetry parameters in a simulation of the measured spectrum gives a pattern that matches closely the pattern observed (Figure 3a). The signal at 10.3 ppm is assigned to aluminum bonded in five-fold coordination, with the signal at 3.1 ppm assigned to aluminum bonded in a highly symmetric octahedron, which was at odds with the original model.

Computational Structural Optimization. The second strategy was to utilize computational modeling to investigate the energetic stability of the proposed model. Starting coordinates were taken from the Rietveld-refined coordinates for Al, P, C, and O and

(34) Brown, I. D.; Altermatt, D. *Acta Crystallogr. B* **1985**, *41*, 244.

Table 1. Atomic Coordinates of AlMePO-2 Derived from Refinement against X-ray Powder Data[a]

atom	*x*	*y*	*z*	$U_i/U_e \times 100$
P(1)	0.8786(3)	0.2179(6)	0.7653(16)	0.69(2)
Al(1)	0.8236(3)	0.3520(6)	0.2735(17)	1.60(2)
Al(2)	0.75	0.0952(11)	0.0262(23)	1.60(2)
O(1)	0.8709(8)	0.3025(15)	−0.0061(30)	1.59(2)
O(2)	0.75	0.4076(21)	0.545(4)	1.59(3)
O(3)	0.8164(5)	0.1211(12)	0.7571(34)	1.59(3)
O(4)	0.8810(7)	0.3107(15)	0.5234(30)	1.59(3)
C(1)	0.9523(8)	0.1377(16)	0.7901(33)	1.59(3)
O(5)	0.8158(5)	0.5212(12)	0.2097(32)	1.59(3)
O(6)	0.75	0.2730(20)	0.131(4)	1.59(3)
H(1)	0.9856(23)	0.205(5)	0.799(28)	
H(2)	0.960(4)	0.082(10)	0.647(14)	
H(3)	0.954(4)	0.081(10)	0.941(15)	

[a] *Pmnb*, $a = 19.7105(1)$ Å, $b = 10.1385(5)$ Å, $c = 5.1408(3)$ Å.

Table 2. Atomic Coordinates of AlMePO-2 Derived from Energy Minimization Using the CASTEP Code[30] [a]

atom	*x*	*y*	*z*
P(1)	0.8768	0.2235	0.7875
Al(1)	0.8215	0.3509	0.2877
Al(2)	0.75	0.0931	0.0377
O(1)	0.8762	0.3149	0.0190
O(2)	0.75	0.4108	0.5534
O(3)	0.8169	0.1296	0.7940
O(4)	0.8764	0.2977	0.5310
C(1)	0.9532	0.1344	0.7926
O(5)	0.8165	0.5227	0.2296
O(6)	0.75	0.2582	0.1821
H(1)	0.9965	0.2015	0.7957
H(2)	0.9569	0.0713	0.6211
H(3)	0.9547	0.0722	0.9652
H(4)[b]	0.8201	0.0548	0.4489
H(5)[b]	0.75	0.8763	0.7715

[a] *Pmnb*, $a = 19.7105$ Å, $b = 10.1385$ Å, $c = 5.1408$ Å. [b] H(4) and H(5) are protons placed for charge balancing at the sites suggested by bond valence sum calculations.

supplemented by methyl hydrogens and protons placed on the locations predicted by bond valence sum calculations. Structural optimization available via computational calculation is well-suited to locating optimum atomic positions. An energy minimization was performed on the proposed model for AlMePO-2. Initially, the proposed uncoordinated water molecule was omitted from the calculation. The result obtained suggested that a hydroxyl group at the triply coordinated oxygen atom would not be stable as the hydrogen atom moved during the optimization process to a position of (0.16, 0.25, −0.05) where it adopted a negative charge, suggesting that this was a preferred position for a hydroxyl group. However, the rest of the framework moved very little during the energy minimization, showing that much of the basic layer structure was plausible. The next step involved inserting an oxygen atom into the structure, at the position (0.16, 0.25, −0.05) suggested by the previous calculation, and repeating the energy minimization procedure with hydroxyl groups at this position and located on one of the original oxygens. This structure optimized with a significantly lower energy of -2.08×10^6 kJ mol^{-1} in comparison to -1.90×10^6 kJ mol^{-1}. In addition, the Al atoms were now in six- and five-coordinate environments, in agreement with the NMR spectroscopy results, and the weight loss during heating to 600 °C could be explained satisfactorily by complete breakdown of the structural hydroxyl groups.

Reevaluation of the Experimental X-ray Powder Diffraction Data. In light of these new insights, the X-ray powder diffraction profile of AlMePO-2 (collected on a second preparation of AlMePO-2 with a very similar X-ray diffraction pattern and similar Al and P MAS NMR) was reinvestigated using the direct methods program EXPO. Using this approach, the position for the oxygen of the hydroxyl group found by computational modeling could be identified and input into the model as an oxygen atom during the procedure. The resulting solution gave a structure for which the intralayer atomic arrangement was in close agreement with the model obtained from the computational approach. Noticeably, however, the offset between adjacent layers (which are symmetry related about an inversion center) was different for this second model.

To determine which stacking arrangement was the better structural model, each was used for a full Rietveld refinement against the X-ray powder diffraction data. In each refinement, soft constraints were placed on the P−O bond lengths, and the methyl protons were held in a staggered conformation with respect to the PO_3 group (in the real structure, the methyl groups would be expected to be rotating very rapidly at room temperature[35]). The first model provided a fit comparable in quality with that of the original analysis [$\chi^2 = 30.52$ (57 variables), with $R_{wp} = 13.42\%$ and $R_p = 10.19\%$]. A slightly better fit to the data [$\chi^2 = 25.24$ (57 variables), with $R_{wp} = 12.19\%$ and $R_p = 8.78\%$) was obtained for the second model (Figure 5). Further evidence to support this structure comes from the computational modeling, which indicates that the second model is slightly more stable [by −0.772 kJ/mol (−0.008 eV)], although the relatively small differences in energies indicate that the bonding between the layers, which is through van der Waals forces, is relatively weak.

The final centrosymmetric *Pmnb* orthorhombic unit cell has dimensions $a = 19.7105(1)$ Å, $b = 10.1385(5)$ Å, and $c = 5.1408(3)$ Å. Bond valence sum calculations indicate that the 12 oxygen atoms on edges shared between AlO_5 and AlO_6 polyhedra each have an attached proton, giving a unit cell composition of $Al_{12}(CH_3PO_3)_8 \cdot O_4 \cdot (OH)_{12}$. This revised structural model is in good agreement with all of the experimental data, and it is in close agreement with the results obtained from energy minimization of the structure (see Tables 1 and 2 for a comparison of experimentally derived coordinates and energy-minimized coordinates).

The structure of $Al_{12}(CH_3PO_3)_8O_4 \cdot (OH)_{12}$ is lamellar, with each aluminophosphonate layer covered on each side by methyl groups. The methyl groups project at an angle to the inorganic layers, in a "herringbone" fashion, and the methyl groups on adjacent layers point in different directions (Figure 6a). The inorganic layers themselves are best considered as being composed of chains of trimers of aluminate polyhedra connected by the apical oxygen of an AlO_6 octahedron (Figure 6b). These parallel chains are themselves connected by methylphosphonate units to give sheets. The aluminum trimer consists of two distorted trigonal AlO_5 bipyramids that share an edge and that also share an edge

(35) Carter, V. J.; Kujanpaa, J.; Riddell, F. G.; Wright, P. A.; Turner, J. F. C.; Catlow, C. R. A.; Knight, K. S. *Chem. Phys. Lett.* **1999**, *313*, 505.

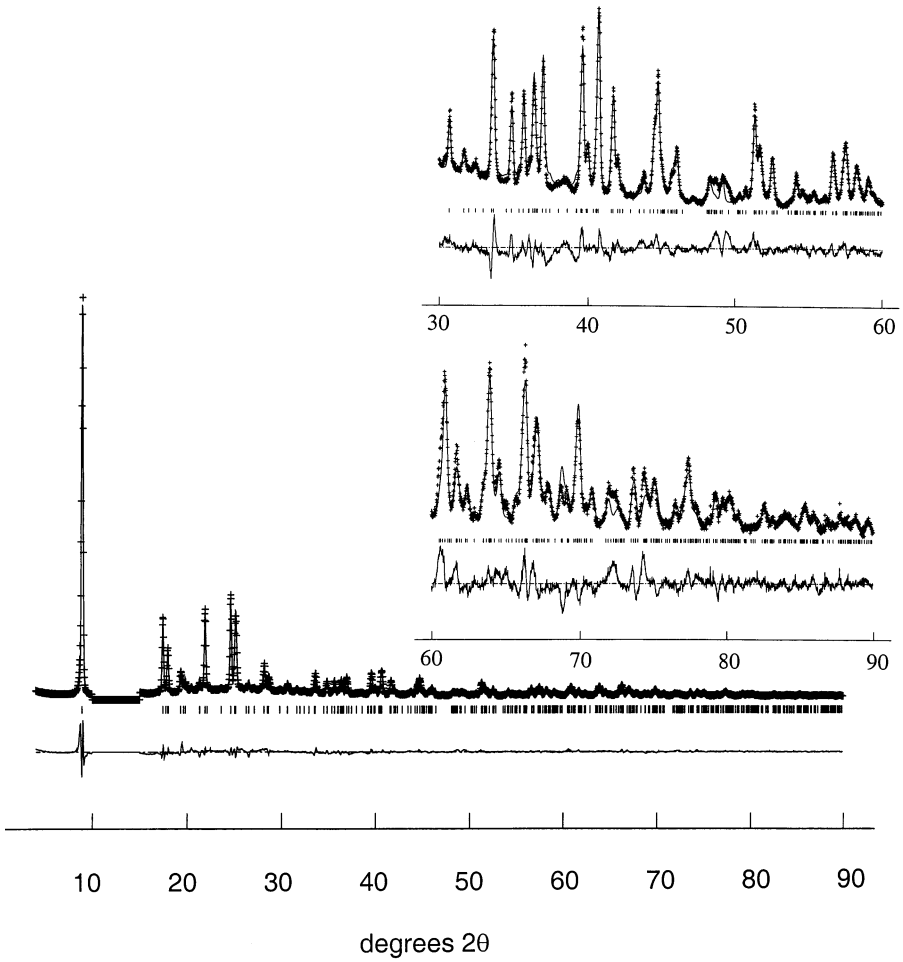

Figure 5. Rietveld-refined X-ray powder profile of AlMePO-2, *Pmnb*, $a = 19.7105(1)$ Å, $b = 10.1385(5)$ Å, $c = 5.1408(3)$ Å, using the asymmetric unit derived from direct methods analysis of the diffraction data in light of computational modeling results [$\chi^2 = 25.24$ (57 variables), with $R_{wp} = 12.19\%$ and $R_p = 8.78\%$]. An impurity peak between 10 and 16° 2θ was excluded.

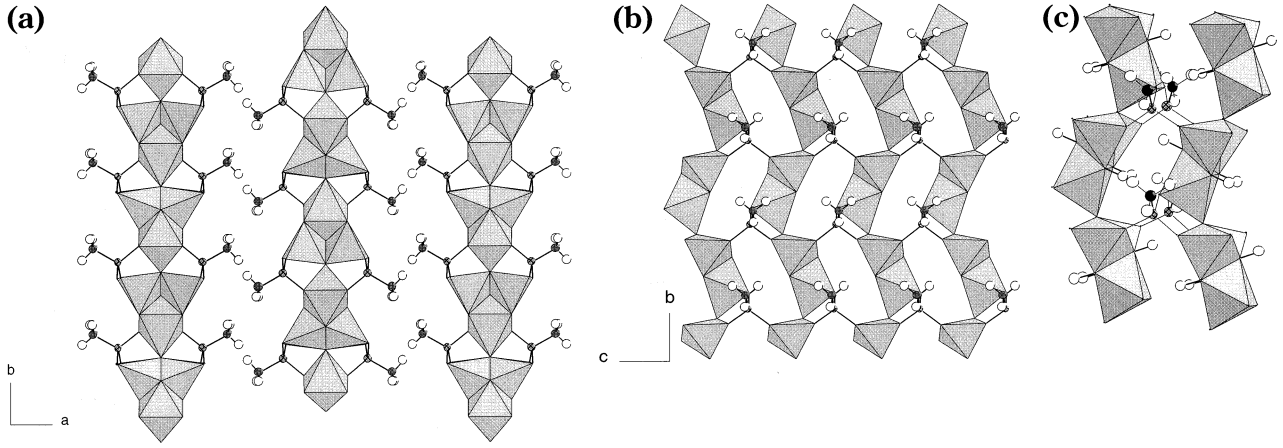

Figure 6. Structure of AlMePO-2, unit cell formula $Al_{12}(CH_3PO_3)_8 \cdot O_4 \cdot (OH)_{12}$, showing (a) the arrangement of lamellae parallel to the *b* and *c* axes and stacked along *a* and the aluminate trimers, consisting of two trigonally bipyramidally coordinated and one octahedrally coordinated aluminum (all edge-sharing), and (b) a view of one of the sheets, showing the chains of aluminate trimers linked by methyl phosphonate groups. The coordinated aluminums are represented by gray polyhedra. Hydroxyl protons, predicted from bond valence calculations and included in the energy minimizations are omitted from parts a and b for clarity, but are shown in part c, which shows an expanded section of a single layer with the smaller white spheres representing the structural hydroxyls and the larger white spheres representing the methyl protons.

each with an AlO_6 octahedron, as indicated by the ^{27}Al NMR spectrum. All of the oxygens on the shared edges of these three aluminum−oxygen polyhedra are thought, on the basis of bond valence calculations and subsequent energy minimization, to be bonded to protons, as shown in Figure 6c. This structural feature is similar to the occurrence of structural hydroxyl groups observed in $Al(OH) \cdot (CH_3PO_3) \cdot H_2O$.[12] Dehydroxylation of the solid, which occurs at 450 °C, results in structural collapse. The oxygen that is connected to three aluminums in

planar trigonal coordination, which links the trimers, is not thought to be bonded to a proton. The presence of edge-sharing trimers of metal polyhedra is reminiscent of the trimer of edge-sharing octahedra observed in the Keggin anion and underlines the "building block" nature of layered and framework solids.[36]

The five-fold coordination reported here, while unusual, has a range of precedents in condensed structures (such as andalusite, Al_2SiO_5) and in framework structures, such as aluminophosphates.[37] Furthermore, recent solid-state NMR spectroscopy studies of an aluminum phenylphosphonate strongly suggest such an environment in that material as well.[38] The trigonal coordination of oxygen by aluminum is also uncommon but has been observed previously, for example, in Al_2TiO_5.[39]

Conclusion

A combination of techniques has enabled the structure of a novel aluminum methylphosphonate with an Al/P ratio of 1.5 to be determined. The structure is lamellar, a typical motif for these organic−inorganic hybrids. The aluminum is found to occupy two environments in the inorganic layer, distorted trigonal bipyramidal and octahedral, that are arranged in edge-sharing trimers. This extends the observed variety in coordination chemistry exhibited by aluminum in the structures of aluminophosphonates. Other notable features include structural hydroxyl groups and an oxygen atom coordinated to three aluminum atoms in a trigonal-planar configuration.

The route by which the structure was solved, in the absence of crystals of sufficient quality for single-crystal diffraction, is of interest. A version of a direct methods approach adapted for X-ray powder diffraction data gave a structural model close to the final solution but unable to match experimental evidence such as the results of ^{27}Al MAS NMR spectroscopy and thermogravimetry. To arrive at the correct answer, it was necessary to use a range of additional techniques. Computational energy minimization calculations enabled us to refine a partial structural solution to give an improved model of the layer structure in agreement with NMR data. In addition, reevaluation of the experimental X-ray powder diffraction data using the direct methods program gave a layer structure that is similar to that obtained from computer energy minimization calculations. XRD and energy calculations are able to discriminate between alternative layer stacking models for the structure, which differed only in the offset of the layers perpendicular to the direction of stacking ($^1/_2 - x$, $^1/_4 + y$, z), ultimately giving the preferred model described.

Acknowledgment. We acknowledge the EPSRC for financial support (M.E. and P.G.), as well as Sylvia Williamson for performing the CHN analysis. P.A.C. and P.G. are grateful for the provision of computer time at the U.K. Computational Chemistry Facility at the Rutherford-Appleton Laboratory. The EPSRC solid-state NMR facility is acknowledged for the ^{13}C and ^{31}P MAS NMR data.

CM011296Q

(36) Draznieks, C. M.; Newsam, J. M.; Gorman, A. M.; Freeman, C. M.; Férey, G. *Angew. Chem., Int. Ed.* **2000**, *39*, 2270.

(37) Loiseau, T.; Mellot-Draznieks, C.; Sassoye, C.; Girard, S.; Guillou, N.; Huguenard, C.; Taulelle, F.; Férey, G. *J. Am. Chem. Soc.* **2001**, *123*, 9642.

(38) Chaplais, G.; Prouzet, E.; Flank, A. M.; Le Bideau, J. *New J. Chem.* **2001**, 25, 1265.

(39) Morosin, B.; Lynch, R. W. *Acta Crystallogr. B* **1972**, *28*, 1040.